Bull. Mater. Sci., Vol. 37, No. 3, May 2014, pp. 563–569. © Indian Academy of Sciences.

High temperature magnetic properties of nanocrystalline $Sn_{0.95}Co_{0.05}O_2$

O MOUNKACHI[1], E SALMANI[2], M BOUJNAH[2], H LABRIM[3], H EL MOUSSAOUI[1,2], M HAMEDOUN[1,*], A BENYOUSSEF[1,2], A EL KENZ[2], H EZ-ZAHRAOUY[2], R MASROUR[4] and E K HLIL[5]

[1]The Institute for Nanomaterials and Nanotechnology, MAScIR (Moroccan Foundation for Advanced Science, Innovation and Research), Rabat, Morocco
[2]LMPHE (URAC 12), Departement of Physique, BP 1014, Faculty of Science, Mohammed V-Agdal University, Rabat, Morocco
[3]National Centre for Energy, Sciences and Nuclear Techniques, CNESTEN, Morocco
[4]Laboratory of Materials, Processes, Environment and Quality, Cady Ayyed University, National School of Applied Sciences, Safi, Morocco
[5]Institut Néel, CNRS et Université Joseph Fourier, BP 166, F-38042 Grenoble Cedex 9, France

MS received 17 October 2012; revised 17 December 2012

Abstract. Structural and magnetic properties of $Sn_{0.95}Co_{0.05}O_2$ nanocrystalline and diluted magnetic semiconductors have been investigated. This sample has been synthesized by co-precipitation route. Study of magnetization hysteresis loop measurements infer that the sample of $Sn_{0.95}Co_{0.05}O_2$ nanoparticle shows a well-defined hysteresis loop at 300 K temperature, which reflects its ferromagnetic behaviour. We confirmed the room-temperature intrinsic ferromagnetic (FM) semiconductors by *ab initio* calculation, using the theory of the functional of density (DFT) by employing the method of Korringa–Kohn–Rostoker (KKR) as well as coherent potential approximation (CPA, explain the disorder effect) to systems. The ferromagnetic state energy was calculated and compared with the local-moment-disordered (LMD) state energy for local density approximation (LDA) and LDA–SIC approximation. Mechanism of hybridization and interaction between magnetic ions in $Sn_{0.95}Co_{0.05}O_2$ is also investigated. To explain the origin of ferromagnetic behaviour, we give information about total and atoms projected density of state functions.

Keywords. Diluted magnetic semiconductors; ferromagnetic, SnO_2; *ab-initio* calculation; KKR–CPA; spintronic.

1. Introduction

Synthesis of diluted magnetic semiconductors (DMS) obtained by doping magnetic transition elements such as Mn, Fe and Co into nonmagnetic semiconductors is one of the most active topics in the spintronics field, which is considered as an alternative to the traditional semiconductor electronics (Ohno 1998; Prinz 1998). Study of spintronic materials has been stimulated by theoretical development, which has shown that wide-band-gap semiconductors are the most promising candidates for achieving high Curie temperatures (T_C) (Dielt *et al* 2000). One of the goals of recent intense research in the field of magnetic materials is to obtain room-temperature intrinsic ferromagnetic (FM) semiconductors. However, numerous studies performed on these systems have led to a controversy on the nature (intrinsic or extrinsic) of the ferromagnetism in these systems. These include Co-doped TiO_2 (Matsumoto *et al* 2001), Cr-doped AlN (Wu *et al* 2003), Fe-doped (Han *et al* 2002), V-doped (Saeki *et al* 2001) and Co-doped ZnO (Belghazi *et al* 2006). Among promising host materials for diluted magnetic semiconductor (DMS) systems, SnO_2 have attracted considerable attention due to a number of unusual magneto-optical, electronic and magnetic properties, including a magnetically tunable bandgap, resulting from large *sp–d* exchange interaction between the magnetic ions and the band electrons. Tin dioxide (SnO_2) is an *n*-type semiconductor with a crystalline structure of the rutile type. It is a semiconductor with wide-band-gap, around 3·6 eV (Cho *et al* 2002; Fang *et al* 2008), and its optical and electrical properties are widely used in technological applications such as in solar cells, gas sensing (Hidalgo *et al* 2005), transparent electrodes (Lalauze *et al* 1987) and optoelectronic devices (Vishwakarma *et al* 1993). As we all know, doping can improve the performance of SnO_2. Many results have been reported on Fe (Fitzgerald *et al* 2004; Punnoose *et al* 2005), Co (Hong *et al* 2005a; Hong and Sakai 2005; Srinivas *et al* 2009; Bagheri 2010), Ni

*Author for correspondence (hamedoun@gmail.com)

(Hong *et al* 2005), Mn-doped (Wang *et al* 2008; Liu *et al* 2009) SnO_2 oxides. Coey *et al* (2004) found ferromagnetic stability in Fe-doped SnO_2 thin film with moments ranging from 1·06 to 4.76 μ_B/Fe. Many works and conflicting results for ferromagnetic properties of Co-doped SnO_2, Ogale *et al* (2003) reported high temperature ferromagnetism with giant magnetic moment in transparent Co-doped $SnO_{2-\delta}$, ferromagnetic properties at room temperature was observed by Fitzgerald *et al* (2006) for Co-doped thin. Nevertheless, ferromagnetism is much more difficult to find and understand (intrinsic or extrinsic). Experimentally, the prediction of high temperature ferromagnetism depends on many experimental parameters: preparation methods, measurement techniques, substrate chooses, unexpectedly carriers introduced during the synthesis, for example, H or O and acceptor or donor defects. Especially in Co-doped SnO_2 polycrystalline sample compared to Co-doped thin film, a room-temperature ferromagnetism was observed in nanocrystalline $Sn_{0.95}Co_{0.05}O_2$-based diluted magnetic semiconductors less than 5% of Co (Srinivas *et al* 2009). The theoretical prediction of room temperature ferromagnetism in Co-doped SnO_2 was made by Rahman *et al* (2008) and Zhang and Yan (2009) using *ab-initio* calculation with GGA or LDA approximation without SIC correction.

In the present study, Co-doped SnO_2 nanocrystalline was synthesized by the co-precipitation method. The structure and gain sizes of the samples were evaluated using X-ray diffraction. Magnetic properties of the products were characterized with a superconducting quantum interference device (SQUID) to determine magnetization hysteresis and magnetization as a function of temperature. ZFC/FC measurements were carried out in the temperature range of 5–360 K with an applied field of 500 Oe. To explain the mechanism of origin of ferromagnetism in Co-doped SnO_2, we have performed *ab initio* calculations using the KKR–CPA method. The ferromagnetic states (FM) energy was calculated and compared with the local-moment-disordered (LMD) state energy for LDA (local density approximation) and LDA–SIC approximation. Mechanism of hybridization and interaction between magnetic ions in $Sn_{0.95}Co_{0.05}O_2$ are also investigated.

2. Experimental

2.1 *Experimental procedure*

The simple solution of SnO_2 doped cobalt was prepared by a simple chemical co-precipitation method using $SnCl_2{\cdot}2H_2O$ and $CoCl_2{\cdot}6H_2O$, as the sources of Sn and Co, respectively. The precursors were added in H_2O and mixed homogeneously and refluxed under air atmosphere to yield a uniform mixture of precursor at 80 °C for 30 min, The pH of the solution was constantly monitored as the NaOH solution was added drop-wise. The dropping rate must be well controlled for the chemical homogeneity. The reactants were constantly stirred using a magnetic stirrer until a pH level of > 12 was achieved. The precipitates were washed several times to remove the water-soluble impurities and free reactants and dried. The spongy contents were filtered, dried and then powdered. Heating treatments of the synthesized powders were realized at 800 °C for 8 h. The crystal structure and particle size of the samples were determined using a Bruker-AXS D8 ADVANCE X-ray diffractometer (XRD) with CuKα radiation ($\lambda = 0{\cdot}15406$ nm), while the magnetic characterization was done by magnetic properties measurement system (MPMS SQUID VSM Quantum design).

2.2 *X-ray diffraction pattern*

Figure 1 shows X-ray pattern diffraction of Co-doped SnO_2 ($Sn_{0.95}Co_{0.05}O_2$). The positions and relative intensities of all the peaks indicate that the crystalline structure of the products favours the formation of rutile phase, which is accordant to JCPDS card No. 82-0514 for SnO_2. The crystallite sizes of the produced $Sn_{0.95}Co_{0.05}O_2$ for the most intense peak (211) plane estimated from the X-ray diffraction data using the Debye–Scherrer formula:

$$d_{RX} = \frac{K\lambda}{\beta \cos\theta},$$

where d_{RX} is the crystallite size, $k = 0{\cdot}9$ the correction factor to account for particle shapes, $\lambda = 1{\cdot}5406$ Å the wavelength of Cu, β the full width at half maximum (FWHM) of the most intense diffraction peak (211) plane and θ is the Bragg angle. The average value of the crystallites dimension for two samples was found to be 21·14 nm.

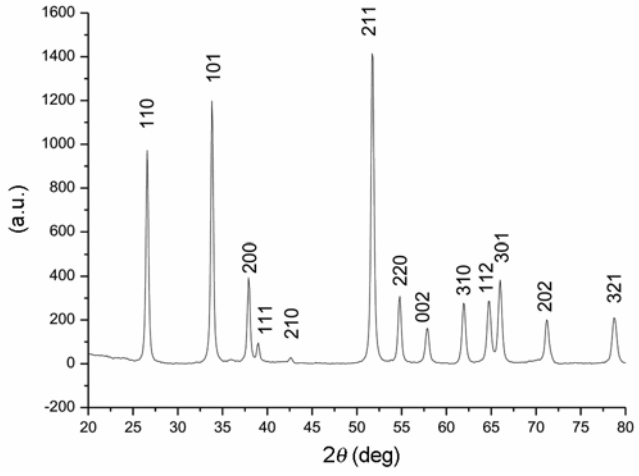

Figure 1. X-ray diffraction pattern for $Sn_{0.95}Co_{0.05}O_2$ nanocrystalline.

2.3 *Magnetic measurements*

The magnetic properties of $Sn_{0.95}Co_{0.05}O_2$ nanocrystalline have been studied by measuring the magnetization as a function of temperature in applied field of 500 Oe. The zero field-cooled (ZFC) and field-cooled (FC) curves are shown in figure 2, which have low magnetic anisotropy of SnO_2-doped cobalt. The corresponding Curie temperature is higher than room temperature. Figure 3 shows magnetic field dependence of magnetic moment at 5 K and room temperature (300 K) of $Sn_{0.95}Co_{0.05}O_2$. The hysteresis loops close at low field and the magnetization seems to approach saturation at ~10 kOe, especially, at room temperature. The saturation moment is (M_s = 0·18 emu/g; M_s = 0·095 μ_B/Co) and the coercive field is (H_c = 7 Oe) measured at room temperature (300 K). Like this magnetic character was observed in same DMS nanoparticule in Co-doped SnO_2 (Srinivas *et al* 2009) and Co-doped ZnO (Pal and Gir 2011) by simple doping method or by co-doping method (Mounkachi *et al* 2012). Indeed, figure 4 shows a plot of inverse d.c. magnetic susceptibility ($1/\chi$ = H/M) as a function of temperature for Co-doped SnO_2. As can be seen from this figure, the plot follows a linear Curie–Weiss type behaviour, $\chi = C/[T - \theta]$. The inverse d.c. magnetic susceptibility ($1/\chi$ = H/M) varies linearly with the temperature, following Curie–Weiss type behaviour, $\chi = C/[T - \theta]$. This means that the magnetic impurities (Co) are coupled ferromagnetically. The appearance of ferromagnetism in the pristine Co-doped SnO_2 nanocrystalline may be attributed to effective exchange interactions between magnetic impurities (cobalt) or by unpaired electron spins originating from the surface defects such as oxygen vacancy clusters instead of single neutral oxygen vacancies

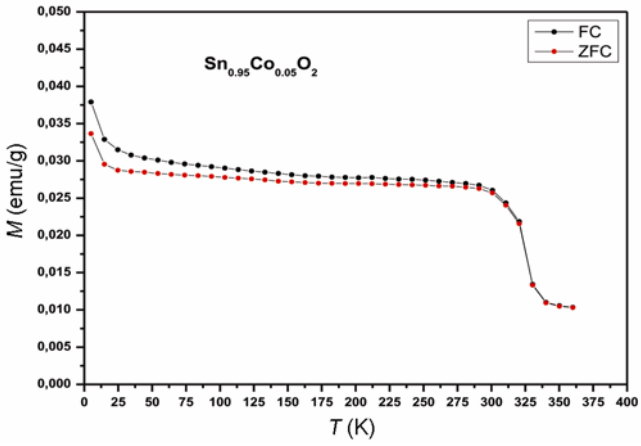

Figure 2. Magnetization vs temperature measured on a $Sn_{0.95}Co_{0.05}O_2$ nanocrystalline at external magnetic field of 500 Oe.

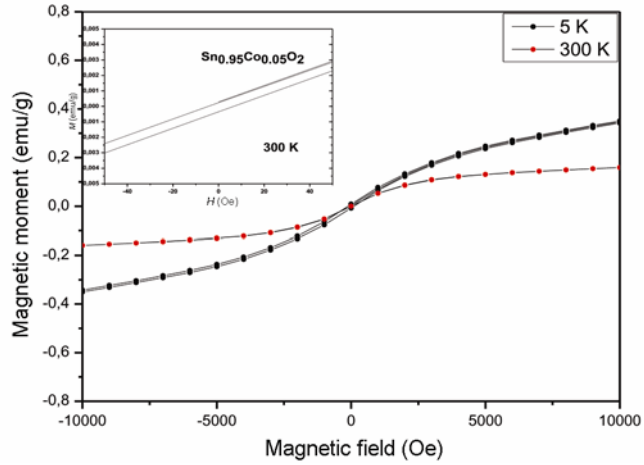

Figure 3. Magnetic hysteresis loops of $Sn_{0.95}Co_{0.05}O_2$ nanocrystalline at temperatures 5 and 300 K.

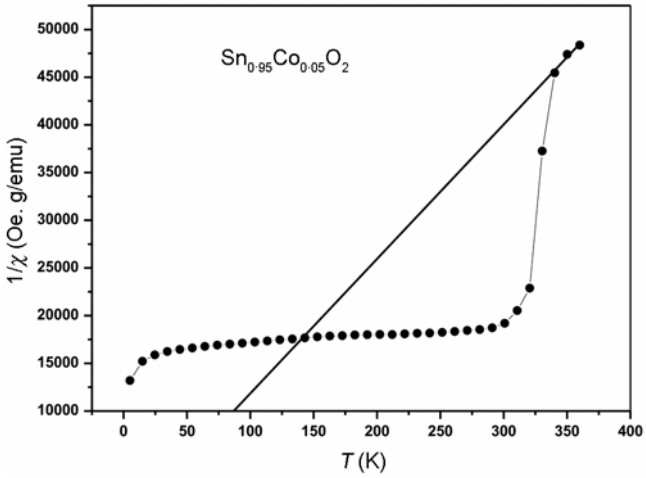

Figure 4. Inverse magnetic susceptibility vs temperature for $Sn_{0.95}Co_{0.05}O_2$ nanocrystalline.

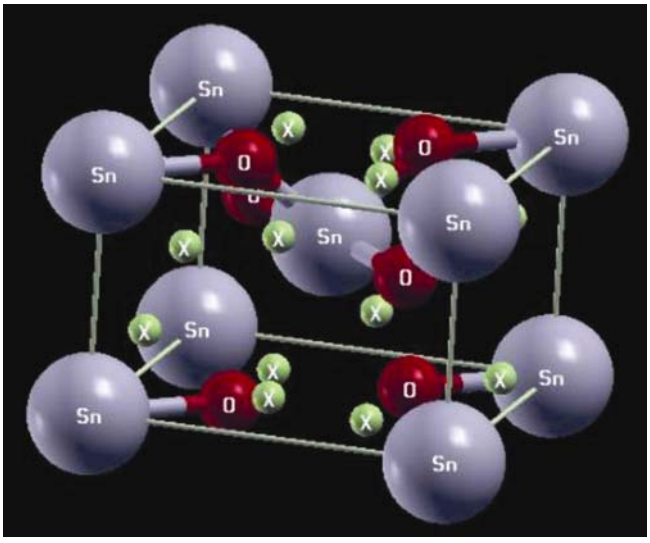

Figure 5. SnO_2 in rutile structure.

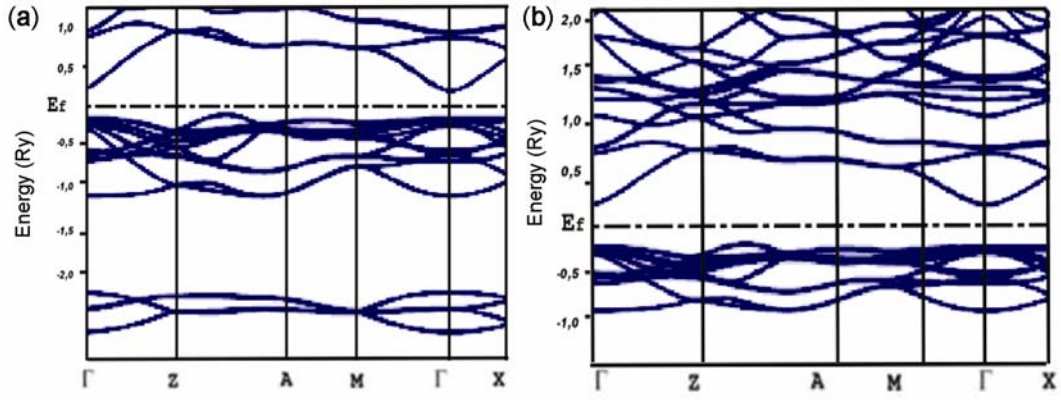

Figure 6. Band structure calculation of SnO_2 with (**a**) LDA approximation and (**b**) LDA–SIC approximation.

or by secondary phases. In the case of Co-doped SnO_2 samples, the origin of ferromagnetism is very complex. Although, different mechanisms might be responsible, in this case we use *ab-initio* calculation to understand this ferromagnetic stability. In our investigation, since the above structural characterizations have ruled out the presence of secondary phases including Co clusters, the observed ferromagnetism should be the intrinsic nature of the Co-doped SnO_2 that we confirmed with electronic structure calculation.

3. Theoretical investigation

In the present work, the electronic structure has been calculated from *ab-initio* calculation, using the theory of the functional of density (DFT) by employing the method of Korringa–Kohn–Rostoker (KKR) as well as the coherent potential approximation (CPA, explain the disorder) to systems. CPA method is mean field theory and supposed to be effective medium which describes the configuration average of the electronic structure of a substitution alloy. The effective medium is calculated self-consistently usually within the single site approximation. SnO_2 has a tetragonal symmetry in rutile structure (figure 5). The rutile structure is characterized by two lattice parameters $a = 4{\cdot}73$ Å and $c = 3{\cdot}18$ Å computed from our experimental data. It is worth noting that for each atom the sphere radius is taken such that the volume of the unit cell is the sum of the volumes of the all atomic spheres. In order to achieve a good packing, we should add initially 'empty' spheres (ES) with ($Z = 0$) representing atomic inter-sites. Using the space group $P4_2/mnm$ in the international tables of X-ray crystallography table N° 136, we put the six atoms, two tin atoms occupying 2a Wyckoff positions: (0, 0, 0) (1/2, 1/2, 1/2) and four oxygen ions occupying 4*f* positions: (u, u, 0) ($-u$, $-u$, 0) (1/2 + u, 1/2 – u, 1/2) (1/2 – u, 1/2 + u, 1/2), while a set of eight ES has been localized at the positions: (1/2, 0, 0·1682) (0, 1/2, –0·1682) (0, 1/2, 0·1682) (1/2, 0, 0·1682) (–0·3125, 0.3125, 0) (–0·1875, –0·1875, 0) (0·1875, 0·1875, 0), (0·3125, –0·3125, 0). This atomic configuration is presented in figure 5.

In order to explain the mechanism of ferromagnetism in $Sn_{0.95}Co_{0.05}O_2$, we have performed *ab initio* calculations using the KKR–CPA method, with the parameterization of Vosko (1980). Co impurities are introduced randomly into cation sites of the SnO_2 semiconductor. To solve the DFT one-particle equations, we use multiple scattering theory, i.e. the KKR Green's function (KKR–GF) method for the dilute impurity limit and the KKR coherent–potential approximation (KKR–CPA includes the disorder in calculations) for concentrated alloys. The form of the crystal potential is approximated by a muffin-tin potential, and the wave functions in the respective muffin-tin spheres were expanded in real harmonics up to $l = 2$, where l is the angular momentum quantum number defined at each site. We use higher K-points up to 456 in the irreducible part of the first Brillouin zone. In the present calculations, we used the KKR–CPA code MACHIKANEYAMA2008v08 package produced by Akai of Osaka University (Akai). In figures 6 (for band structure calculation) and 7 (for density of stat calculation), we show the band structure of bulk SnO_2, a bandgap of 2·05 eV for LDA approximation and 3·40 eV for LDA-SIC approximation close to experimental value (Cho *et al* 2002; Fang *et al* 2008). As already known, SnO_2 is a direct bandgap semiconductor ($E_{\Gamma-\Gamma}$), with the lowest energy electron–hole transition occurring at the Γ point. It is interesting to compare the present results with previous band structure calculations. The energy band structure of SnO_2 consists of four bands. The low energy bands, between –1·2 and –1·6 Ry are composed mainly of the semi-core Sn-4*d* states, the next band is the wide valence band within the energy interval from –0·8 to 0·0 Ry consists of the hybridized O–2*p* Sn–5*p* states and has three sub-bands. The conduction band which is higher on energy in the electron spectrum is built of the 5*s* states of tin, which are typical for SnO_2 as well as with the results of past calculations.

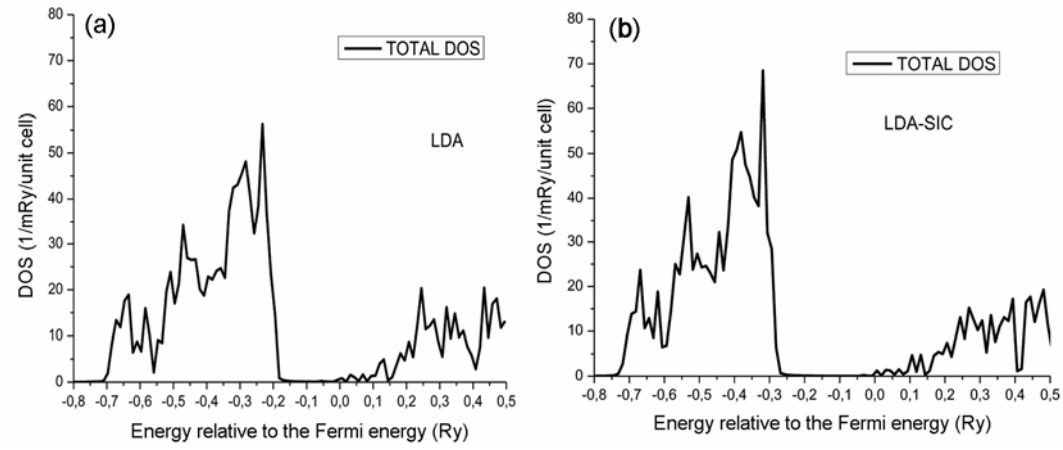

Figure 7. Total density of states of SnO_2 for: (**a**) LDA calculation and (**b**) LDA–SIC approximation.

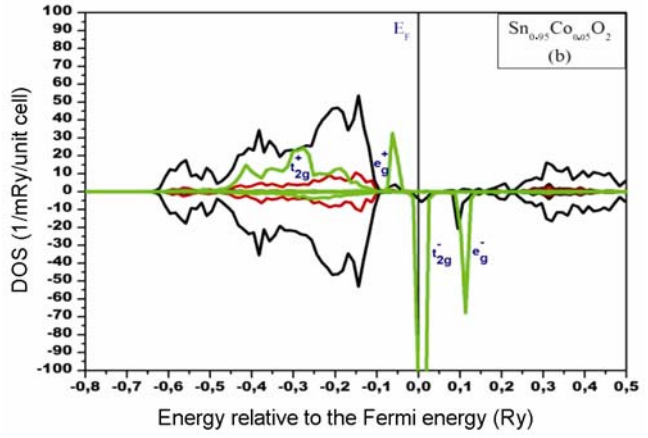

Figure 8. Total and partial density of states of ferromagnetic $Sn_{0.95}Co_{0.05}O_2$ for LDA calculation.

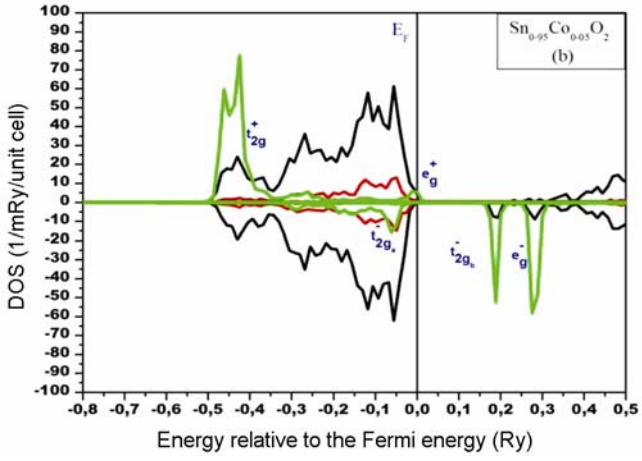

Figure 9. Total and partial density of states of ferromagnetic $Sn_{0.95}Co_{0.05}O_2$ for LDA–SIC calculation.

Table 1. Calculated magnetic moments (total and partial) in $Sn_{0.95}Co_{0.05}O_2$ and energy difference between spin glass and ferromagnetic state.

Co-doped SnO_2	M (μ_β)	M^{Co} (μ_β)	M^{O} (μ_β)	ΔE (meV)
LDA	0·20	3·54	0·01	5·26
LDA–SIC	0·18	3·39	0·00	5·08

We study the magnetic properties of SnO_2, doped in Sn positions with 5% of single transition elements TM, which are Co, in order to compare with our experimental observations. Doping with 5% of Co ion can change the magnetic property of SnO_2. The result of magnetism in $Sn_{0.95}Co_{0.05}O_2$ is illustrate in table 1, which shows that the Co-doped SnO_2 have magnetic moments which are 3·54 μ_B with LDA, but when we add the SIC correction the magnetic moments are 3·39 μ_B. However, the magnetic moments per cobalt ion, calculated from the magnetization data is $M_s = 0{\cdot}095\ \mu_B$/Co for 300 K and $M_s = 0{\cdot}18\ \mu_B$/Co for 5 K, for low temperature comparable to the theoretical calculation (table 1).

In order to determine the most stable magnetic state, the energy difference between the

$$\Delta E = E \text{ (spin-glass state)} - E \text{ (ferromagnetic state)},$$

ferromagnetic state (FM) and disordered local moment (DLM) have been calculated. DLM state describes the spin-glass state at finite temperature where the directions of all local moments are randomly distributed, so that the average magnetization vanishes. The variation of the ΔE as a function of LDA approximations (LDA and LDA–SIC) are given in table 1, in which it is shown that ΔE has always positive values with LDA and LDA–SIC. These indicate that the ferromagnetic state is more stable than the spin glass for both cases, and it is correlated with our and author experimental results (Ogale *et al* 2003; Coey *et al* 2004; Srinivas *et al* 2009) and with theoretical results (Wang *et al* 2007, 2008). In order to understand and to explain the more stabilized ferromagnetism state in $Sn_{0.95}Co_{0.05}O_2$, the density of states (DOS) of this system for LDA without and within SIC was calculated and they are presented in figures 8 and 9 within LDA and

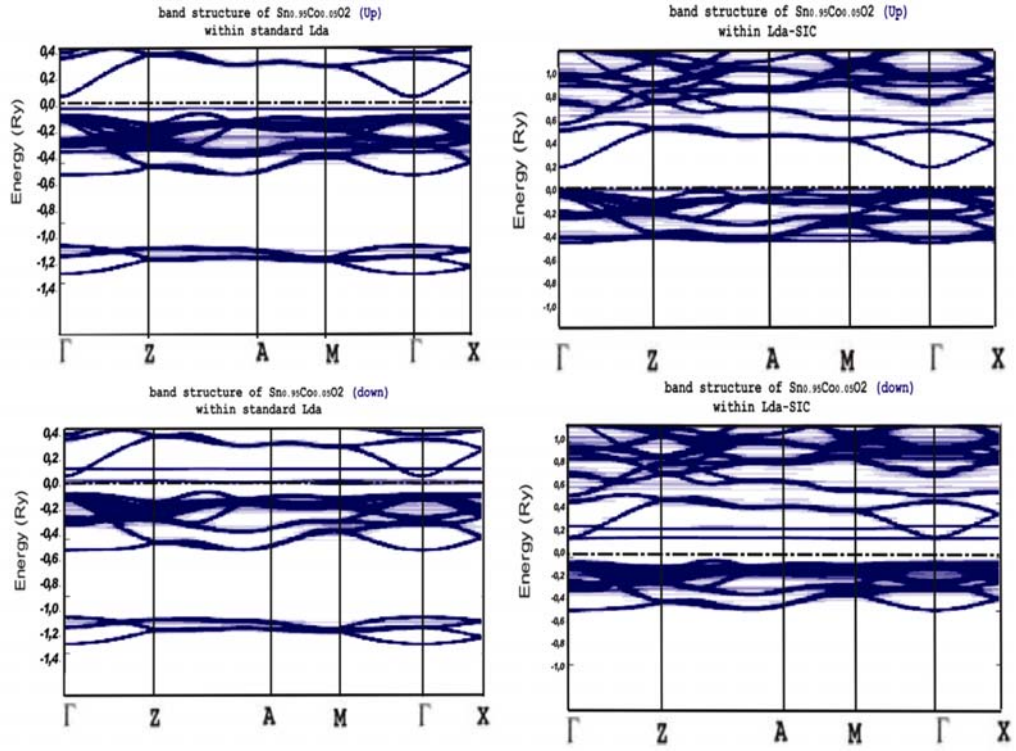

Figure 10. Band structures calculation for spin-up and spin-down of $Sn_{0.95}Co_{0.05}O_2$ within LDA and LDA-SIC approximation, in comparison with pure SnO_2.

LDA-SIC, respectively. In Co ion-doped rutile SnO_2, O ions around Co ions form an octahedral crystal field, splitting *d* orbitals into lower t_{2g} states and upper e_g states as indicated in figure 8 (for LDA approximation). The five electrons in 3*d* are occupied with 3 spins up in t_{2g} state and 2 spin up in e_g state, the exchange splitting between t_{2g} states is larger than the crystal field spitting between t_{2g} and e_g states in Co-doped SnO_2. Besides from figure 8, when we add SIC correction to LDA, we observed the modification of arrangement in electronic structure, such that we obtain 4 electrons in t_{2g} state instead of 3 electrons, with 3 is on spin up, is 1 on spin down, and the remaining 1 is on spin up in e_g state, which leads to Jahn-Teller effect. Indeed, after the rule of Jahn Teller effect, the t_{2g} states for down and up-spin side are leading to the formation of t_{2g} fractions, is indicate in figure 9. Figure 10 shows the band structures calculation for spin-up and spin-down of $Sn_{0.95}Co_{0.05}O_2$ within LDA and LDA-SIC approximation, in comparison with pure SnO_2. The band structures of $Sn_{0.95}Co_{0.05}O_2$ changed a lot with SIC approximation compared with LDA approximation, the bandgaps became smaller than that of pure SnO_2 for LDA approximation, and larger than SnO_2 with SIC approximation (figure 6).

4. Conclusions

This paper describes the synthesis of $Sn_{0.95}Co_{0.05}O_2$ nanocrystalline using a co-precipitation method. XRD spectrum is in good agreement with the standard peak position of SnO_2 (JCPDS card no. 82-0514), without any secondary phase. Magnetic measurement showed that the samples are ferromagnetic at room temperature, well-defined hysteresis loop at 300 K temperature. Based on first-principles spin-density functional calculations, using the Korringa–Kohn–Rostoker method (KKR) combined with the coherent potential approximation (CPA). The ferromagnetic state energy was calculated and compared with the local-moment-disordered (LMD) state energy for LDA (local density approximation) and LDA–SIC approximation. Mechanism of hybridization and interaction between magnetic ions in $Sn_{0.95}Co_{0.05}O_2$ are also investigated.

References

Akai H http://sham.phys.sci.osaka-u.ac.jp/~kkr/

Bagheri M M, Mohagheghi and Shokooh-Saremi M 2010 *Physica* **B405** 4205

Belghazi Y, Schmerber G, Colis S, Rehspringer J L, Berrada A and Dinia A 2006 *Appl. Phys. Lett.* **89** 122504

Cho Y M, Choo W K, Kim H, Kim D and Ihm Y E 2002 *Appl. Phys. Lett.* **80** 3358

Coey J M D, Douvalis A P, Fitzgerald C B and Venkatesan M 2004 *Appl. Phys. Lett.* **84** 1332

Dielt T, Ohno H, Matsukura F, Cibert J and Ferrand D 2000 *Science* **287** 1019

Fang L M, Zu X T, Li Z J, Liu C M, Wang L M and Gao F 2008 *J. Mater. Sci. Mater. Electron.* **19** 868

Fitzgerald C B, Venkatesan M, Douvalais A P, Huber S, Coey J M D and Bakas T 2004 *Appl. Phys. Lett.* **95** 7390
Fitzgerald C B *et al* 2006 *Phys. Rev.* **B74** 115307
Han S J *et al* 2002 *Appl. Phys. Lett.* **81** 4212
Hidalgo P, Castro R H R, Coelho A C V and Gouvea D 2005 *Chem. Mater.* **17** 4149
Hong N H and J Sakai 2005 *Physica* **B358** 265
Hong N H, Ruyter A, Prellier W, Sakai, J. and Huong N T 2005 *J. Phys.: Condens. Matter* **17** 6533
Hong N H, Sakai J, Prellier W and Hassini A 2005 *J. Phys.: Condens. Matter* **17** 1697
Lalauze R, Le Theisse J C, Pijolat C and Soustelle M 1987 *Solid State Ionics* **12** 453
Liu S J, Liu C Y, Juang J Y and Fang H W 2009 *J. Appl. Phys.* **105** 013928
Matsumoto Y *et al* 2001 *Science* **291** 854
Mounkachi O *et al* 2012 *J. Magn. Magn. Mater.* **324** 1945
Ogale S B *et al* 2003 *Phys. Rev. Lett.* **91** 077205
Ohno H 1998 *Science* **281** 951
Pal B and Gir P K 2011 *J. Nanosci. Nanotechnol.* **11** 1
Prinz G A 1998 *Science* **282** 1660
Punnoose A *et al* 2005 *Phys. Rev.* **B72** 054402
Rahman G, Garćıa-Súarez V M and Hong S C 2008 *Phys. Rev.* **B78** 184404
Saeki H, Tabata and Kawai T 2001 *Solid State Commun.* **120** 439
Srinivas K, Vithal M, Sreedhar B, Manivel Raja M and Venugopal Reddy P 2009 *J. Phys. Chem.* **C113** 3543
Vishwakarma S R, Rahmatullah and Prasad H C 1993 *J. Phys.* **D26** 959
Vosko S H, Wilk L and Nusair M 1980 *Can. J. Phys.* **58** 1200
Wang X L, Dai Z X, Zeng 2008 *J. Phys.: Condens. Matter* **20** 045214
Wang X L, Zeng Z, Zheng X H and Lin H Q 2007 *J. Appl. Phys.* **101** 09H104
Wu S Y *et al* 2003 *Appl. Phys. Lett.* **82** 3047
Zhang C W and Yan S S 2009 *J. Appl. Phys.* **106** 063709